ISIJ International, Vol. 55 (2015), No. 2, pp. 441–447

Improvement on Heat Release Performance of Direct-contact Heat Exchanger Using Phase Change Material for Recovery of Low Temperature Exhaust Heat

Takahiro NOMURA, Masakatsu TSUBOTA, Noriyuki OKINAKA and Tomohiro AKIYAMA*

Center for Advanced Research of Energy and Materials, Faculty of Engineering, Hokkaido University, Kita 13 Nishi 8, Kita-ku, Sapporo, 060-8628 Japan.

(*Received on July 31, 2014; accepted on September 22, 2014*)

Latent heat storage using a phase change material (PCM) is a promising method for utilizing the exhaust heat from steelworks. The purpose of this study was to improve the heat release performance of a direct-contact heat exchanger using a PCM and heat transfer oil (HTO). Erythritol (with a melting point of 391 K), which is a kind of sugar alcohol, was selected as a PCM. A vertical stainless steel cylinder with an inner diameter of 200 mm and height of 1 400 mm was used as the heat storage unit (HSU). A ring-shaped injector with 18 holes positioned vertically downward was placed at the bottom of the HSU. Each hole in this injector had a diameter of 2.5 mm. We investigated the effects of the height of the PCM in the HSU, the HTO flow rate, and an increase in the number of injection-nozzle holes on the temperature effectiveness and heat exchange rate as indices of the heat release performances. As results, we found that an increase in the number of nozzle holes accelerated the uniform distribution of the HTO in the liquid PCM, prevented the HTO drift flow and adverse solidification of the PCM, and improved the heat release performance under the condition of a high HTO flow rate.

KEY WORDS: thermal energy storage; phase change material; latent heat storage; heat recovery; exhaust heat.

1. Introduction

Effectively utilizing the huge amount of exhaust heat produced by steelworks is an important problem with great potential for saving energy and reducing CO_2, because the exhaust heat from steelworks accounts for as much as 4% of the primary energy consumed in Japan.[1)] However, it is difficult to use the exhaust heat because 1) most of the exhaust heat is emitted from batch processes and 2) the heat sources are scattered over a plant.[1)] Therefore, technologies that can manage the gap in time and space between a heat source and a heat demand are strongly needed to utilize the exhaust heat from steelworks.

Latent heat storage (LHS) is one of the promising methods for overcoming the difficulties in utilizing the exhaust heat from steelworks. The LHS method is based on the storage and release of latent heat when a phase change material (PCM) undergoes a phase change from solid to liquid and liquid to solid.[2)] LHS mainly has three advantages. First, a PCM has a large heat capacity due to utilizing latent heat, compared with sensible heat storage methods. Second, the PCM can release and store heat at a constant phase changing temperature. Third, the PCM can be used repeatedly since the phase changing process such as melting and solidifying is repeatable. Because of these advantages, LHS has potential as an energy medium to store recovered heat for suitable periods and efficiently transport it over long distances.

A latent heat transportation system (LHTS)[3–7)] using a PCM is very attractive as an LHS application for utilizing the exhaust heat from steelworks. In an LHTS, a latent heat accumulator articulate with a truck is used. This allows the exhaust heat to be compactly stored as latent heat in the PCM and transported over long distances (~20 km) to other places that need heat sources.

A direct-contact heat exchanger (DCHEX), which has an extremely simple structure, is used as a latent heat accumulator for the LHTS. The DCHEX can exchange heat more rapidly than an indirect heat exchanger such as a shell and tube heat exchanger[4)] because of the negligible thermal resistance of the pipe or capsule used for the heat exchange.[8,9)] In addition, a DCHEX can realize a high heat capacity since the accumulator is lightweight as a result of its simple structure with no heat transfer pipe and capsule.

A DCHEX for LHS has been reported from the viewpoint of 1) the material and 2) the performance of the heat exchanger.

Material: The PCM and heat transfer medium (HTM) for the DCHEX have to be immiscible. Tetradecane (melting temperature, T_m: 279 K)-air,[8)] tetradecane (melting temperature, T_m: 279 K)-ethylene glycol water solution,[8,10,11)] n-eicosane-water,[12,13)] sodium acetate trihydrate (T_m: 331 K)-heat transfer

* Corresponding author: E-mail: takiyama@eng.hokudai.ac.jp
DOI: http://dx.doi.org/10.2355/isijinternational.55.441

oil (HTO),[6] erythritol (T_m: 391 K)/HTO,[4,6] and NaOH–Na_2CO_3 (T_m: 559 K)/dibenzyl toluene[14] have been reported as available PCM and HTM combinations for a DCHEX. In particular, erythritol is a promising PCM for recovering exhaust heat from steelworks at temperatures below 473 K because of its high heat capacity and adequate T_m.[15]

Performance of heat exchanger: Various DCHEXs such as the container type,[4] cassette type,[7,16] and vertical cylindrical tank type[2,15,17,18] have been reported. Kaizawa *et al*.[4] performed bench-scale experiments with a container-type DCHEX, using erythritol as the PCM to observe the heat and fluid flows in the container. They clarified the melting and solidifying mechanism of direct-contact heat exchange between the erythritol and HTO, and pointed out that the DCHEX could easily form a dead zone for the heat exchange during both the heat storage and release. Therefore, the position and number of injection holes for the HTO are important. Horibe *et al*.[16] examined a cassette-type DCHEX that had a nozzle plate with HTO injection holes at the bottom of the accumulator using erythritol. They reported that the heat storage and release performance improved when the flow rate of the HTO increases. Our group examined the heat storage[15,18] and release performance[2] of a vertical cylindrical tank type. In particular, in heat release experiments, we clarified that the DCHEX could rapidly, efficiently, and compactly release the latent heat of the PCM under the condition of a uniform HTO flow. On the other hand, an excess HTO flowrate caused a poor heat release performance because of a stagnant zone for heat transfer. Improving the heat transfer with a higher HTO flowrate is important to improve the heat release performance of all DCHEXs.

Therefore, in this study, we investigated the effects of the height of the PCM, the flow rate of the HTO, and an increase in the number of injection-nozzle holes on the temperature effectiveness and heat exchange rate as indices of the heat release performances. A vertical cylinder made of stainless steel with an inner diameter of 200 mm and height of 1 400 mm was used as the heat storage unit (HSU). A ring-shaped injector with 18 holes positioned to point in a downward direction was placed at the bottom of the HSU. Each of these holes had a diameter of 2.5 mm. We found that increasing the number of nozzles accelerated the uniform distribution of the HTO in the liquid PCM, prevented the drift flow of the HTO and adverse solidification of the PCM, and improved the heat release performance.

2. Experiments

2.1. Materials

Table 1 lists the thermophysical properties of erythritol[4,19] and $C_4H_{10}O_4$, which were used as the PCM and HTO, respectively. Sugar alcohols, including erythritol are good PCM candidates because they have large latent heat values and are not toxic or corrosive to structural materials. In particular, erythritol has a larger latent heat than other PCM candidates. Therefore, it is a suitable PCM to recover a low-temperature heat source in the temperature range of 423–473 K. HTO was selected because of its safety and excellent chemical stability even when mixed with erythritol. In should be noted that the density of HTO is lower than erythritol at all temperature ranges.

Table 1. Thermophysical properties of erythritol as PCM and HTO.

Property	Heat transfer oil (HTO)	Erythritol (PCM)
Density ($kg \cdot m^{-3}$)	780	1 480 (at 293 K)[19] 1 300 (at 413 K)[19]
Specific heat ($kJ \cdot kg^{-1} \cdot K^{-1}$)	2.35	1.35 (at 293 K)[19] 2.74 (at 413 K)[6]
Thermal conductivity ($W \cdot m^{-1} \cdot K^{-1}$)	0.14	0.73 (at 293 K)
Viscosity ($kg \cdot m^{-1} \cdot s^{-1}$)	–	0.02895 (at 395 K)[6]
Latent heat ($kJ \cdot kg^{-1}$)		340[19]
Melting temperature (K)	–	391[19]

2.2. Experimental Setup and Procedure

Figure 1 shows a schematic of the experimental setup. The apparatus mainly consisted of a) the heat storage system, which included a heat storage unit (HSU) and tank for separating the overflowing PCM, and b) the HTO circulation and control system, which consisted of an HTO cooler, an HTO buffer tank, an HTO heater, an HTO flowmeter, and a circulation pump.

The HSU was a stainless steel cylinder with an inner diameter of 200 mm, an outer diameter of 204 mm, and a height of 1 400 mm. Ten K-type thermocouples were used to measure the local temperatures of the PCM and HTO in the HSU. Importantly, to measure the HTO temperatures at the inlet, T_{in}, and outlet, T_{out} of the HSU, K-type thermocouples were also used at the inlet and outlet nozzles. The transient temperature variations were recorded at intervals of 5 s using a digital data logger. A ring-shaped injector with 18 holes positioned to point in a downward direction was placed 50 mm above the bottom of the HSU. Each hole had a diameter of 2.5 mm. It should be noted that, to prevent the regurgitation of liquid PCM into the injector due to a difference between the PCM and HTO densities, it is important to point the injector in a downward direction. The details of the HTO circulation and control system are listed in **Table 2**.

Table 3 lists the experimental conditions used in this study. The effects of the HTO flowrate and PCM height were mainly investigated. In addition, the effects of injector parameters such as the size and number of injection holes were also investigated by comparing the results of the present and previous studies.[2]

The heat release experiments were performed using the following procedures:

1) The PCM and HTO in the HSU were heated to a temperature greater than the T_m of the PCM. Then, the temperatures of both the liquid PCM and HTO in the HSU were maintained at approximately 413 K.

2) Valves V01 and V02 in **Fig. 2** were closed, and V03 was open. Then, the HTO was circulated, and its temperature was controlled at 363 K by the HTO circulating and control system.

3) V03 was closed, and V01 and V02 were opened. Then, the HTO flowed into the HSU, and the experiments started.

4) T_{in} was automatically controlled at 363 K by the HTO heater and cooler during the experiments.

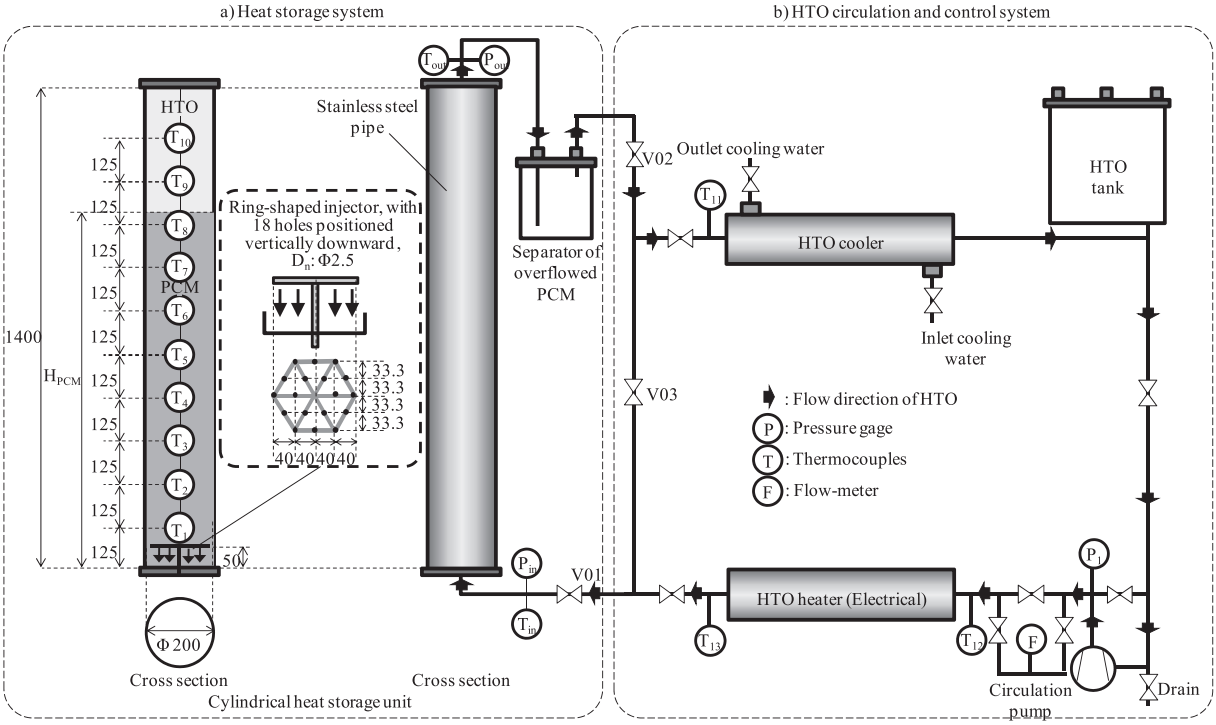

Fig. 1. Schematic diagram of experimental setup for measuring heat exchange rates of direct-contact heat exchanger, a) heat storage system, b) and HTO circulation and control system.

Table 2. Details of devices in HTO circulation and control system.

Item	Specification
HTO cooler	A tubular heat exchanger connected to a chiller circulating coolant water
HTO heater	An electro-thermal type heater with a maximum heating capacity of 12 kW
Flow meter	A rotary flow meter with a range of 2–24 L/min
Circulation pump	A trochoid pump with a maximum flow rate of 20 L/min

Table 3. Experimental conditions of heat release experiments in this study, together with those of previous study for comparative analysis.

Run No.	Mode	$F{\cdot}10^{-5}$	v_n	v_c	Re_n	T_{in}	*PCM*		D	H	D_n	N
		[m^3/s]	[m/s]	[mm/s]	[–]	[K]	M_{PCM} [kg]	H_{PCM} [m]	[m]	[m]	[mm]	[–]
R-1	This study	4.17	0.472	1.33	287	391	27.9	0.6	0.2	1.4	2.5	18
R-2		5.83	0.660	1.86	402	391	27.9	0.6				
R-3		7.50	0.849	2.39	517	391	27.9	0.6				
R-4		4.17	0.472	1.33	287	391	37.2	0.8				
R-5		5.83	0.660	1.86	402	391	37.2	0.8				
R-6		7.50	0.849	2.39	517	391	37.2	0.8				
R-7		8.33	0.943	2.66	574	391	37.2	0.8				
R-8		9.17	1.04	2.92	632	391	37.2	0.8				
R-9		4.17	0.472	1.33	287	391	46.5	1.0				
R-10		5.83	0.660	1.86	402	391	46.5	1.0				
R-11		7.50	0.849	2.39	517	391	46.5	1.0				
Ref. 1	Previous study[2)]	4.17	0.65	1.33	378	391	27.9	0.6	0.2	1.0	3.0	9
Ref. 2		5.00	0.79	1.59	454	391	27.9	0.6				
Ref. 3		5.83	0.92	1.86	530	391	27.9	0.6				
Ref. 4		6.25	0.98	1.99	567	391	27.9	0.6				
Ref. 5		6.67	1.05	2.12	605	391	27.9	0.6				
Ref. 6		7.50	1.18	2.39	681	391	27.9	0.6				

5) The experiments were finished when T_{out} reached approximately T_{in}.

3. Results and Discussion

3.1. Temperature History

Figure 2 shows the changes in the local temperature in the HSU and T_{out} for the various runs: a) R-1: H_{PCM}: 0.6 m, F: $4.17\cdot10^{-5}$ m^3/s, b) R-2 H_{PCM}: 0.6 m, F: $5.83\cdot10^{-5}$ m^3/s, c) R-3, H_{PCM}: 0.6 m, F: $7.50\cdot10^{-5}$ m^3/s. Under all the conditions, three main stages were observed for the local temperature in the PCM zone. First, the temperatures sharply decreased around T_m. Then, they remained constant around T_m. Finally, they decreased and reached approximately T_{in}. The first stage released the sensible heat of the liquid PCM. The second released the latent heat of the PCM, and the third released the sensible heat of the solid PCM.

As shown in Fig. 2(a), which displays the results for a comparatively small F, the temperatures suddenly decreased near the bottom of the HSU after the above-mentioned second stage. This result was the same as the results under the condition where the HTO uniformly flowed in the liquid PCM in a previous study[2] (Run No.: Refs. 1)–3) in Table 3). The previous study[2] clarified that solidified PCM particles sank because of the difference between the densities of the liquid and solid PCM, and finally accumulated at the bottom of the HSU during heat release experiments under the condition that the HTO uniformly flowed in the liquid PCM. The solid PCM was accumulated from the bottom of the HSU. As a result, the temperatures suddenly dropped in order near the bottom of the HSU. The same phenomena were considered to occur in the experiments with a small F.

On the other hand, in Figs. 2(b) and 2(c), which show the results for a comparatively high F, the temperature changes were different from those for smaller F. In the previous heat release experiments,[2] we indicated that a high F caused the formation of a stagnant zone from 1) the drift flow of the HTO and 2) the adverse solidification of the PCM, where a liquid PCM was enclosed in a solid PCM.[12,13] Similar phenomena were considered to occur in these experiments, although the number of injection-nozzle holes and H_{PCM} were different from the previous study.[2]

Figure 3 shows the changes in the local temperatures in the HSU and T_{out} for a) R-4: H_{PCM}: 0.8 m, F: $4.17\cdot10^{-5}$ m^3/s, b) R-5 H_{PCM}: 0.8 m, F: $5.83\cdot10^{-5}$ m^3/s, and c) R-6, H_{PCM}: 0.8 m, F: $7.50\cdot10^{-5}$ m^3/s; and **Fig. 4** shows those for a) R-9: H_{PCM}: 1.0 m, F: $4.17\cdot10^{-5}$ m^3/s, b) R-10 H_{PCM}: 1.0 m, F: $5.83\cdot10^{-5}$ m^3/s, and c) R-11, H_{PCM}: 1.0 m, F: $7.50\cdot10^{-5}$ m^3/s. Similar to Figs. 3(b) and 3(c), the temperature history for a higher F showed a tendency to be further from the results

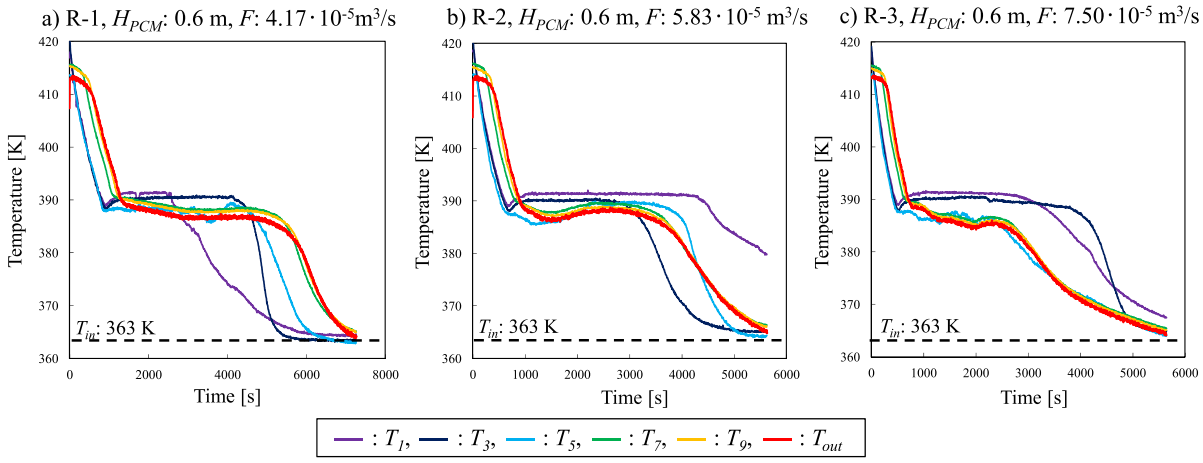

Fig. 2. Changes in local temperature in HSU and T_{out} in a) R-1: H_{PCM}: 0.6 m, F: $4.17\cdot10^{-5}$ m^3/s, b) R-2 H_{PCM}: 0.6 m, F: $5.83\cdot10^{-5}$ m^3/s, and c) R-3, H_{PCM}: 0.6 m, F: $7.50\cdot10^{-5}$ m^3/s. (Online version in color.)

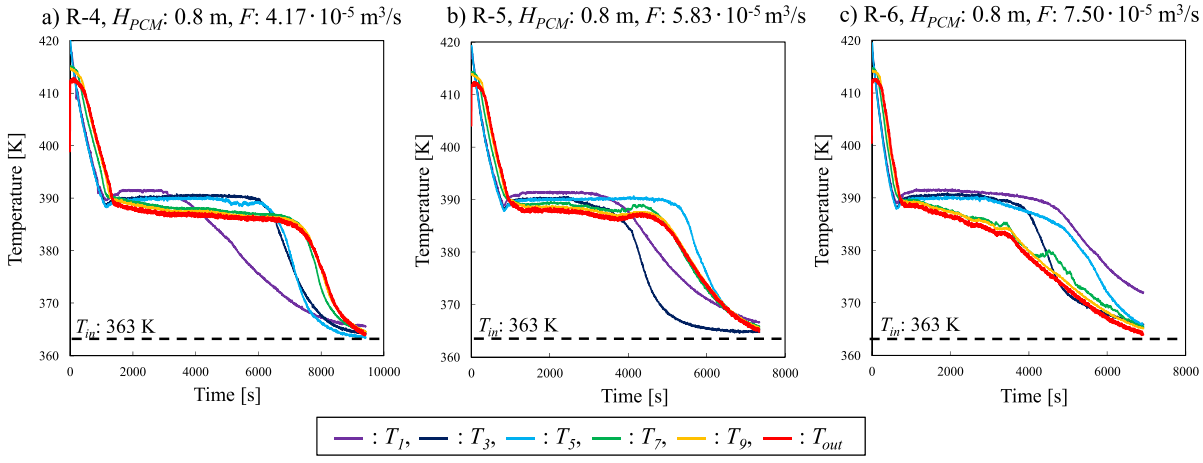

Fig. 3. Changes in local temperature in HSU and T_{out} in a) R-4: H_{PCM}: 0.8 m, F: $4.17\cdot10^{-5}$ m^3/s, b) R-5 H_{PCM}: 0.8 m, F: $5.83\cdot10^{-5}$ m^3/s, and c) R-6, H_{PCM}: 0.8 m, F: $7.50\cdot10^{-5}$ m^3/s. (Online version in color.)

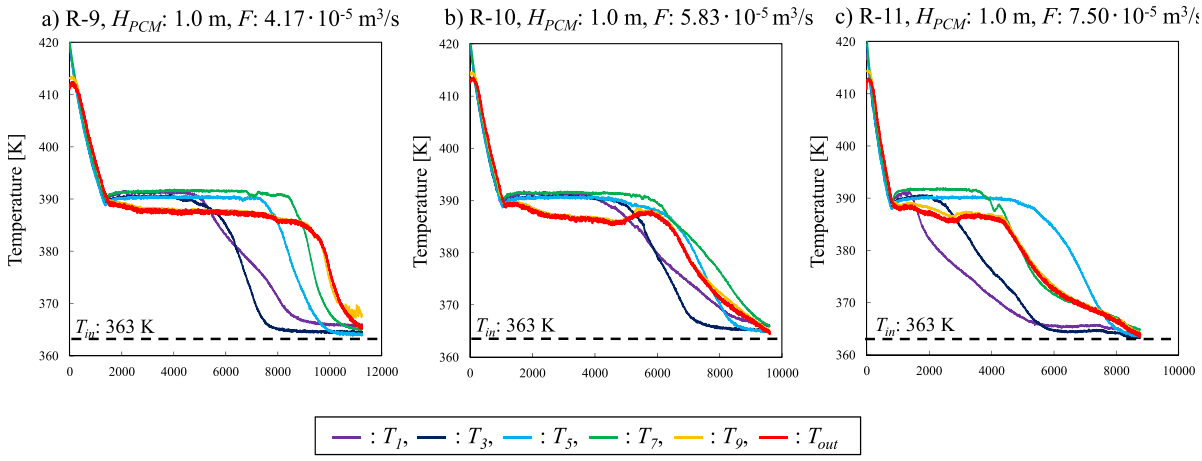

Fig. 4. Changes in local temperature in HSU and T_{out} in a) R-9: H_{PCM}: 1.0 m, F: 4.17·10^{-5} m^3/s, b) R-10 H_{PCM}: 1.0 m, F: 5.83·10^{-5} m^3/s, and c) R-11, H_{PCM}: 0.8 m, F: 7.50·10^{-5} m^3/s. (Online version in color.)

under the condition where the HTO uniformly flowed in the liquid PCM. On the other hand, for a higher H_{PCM}, it was observed that the temperature histories for higher values of F were closer to those under the condition where the HTO uniformly flowed in the liquid PCM. This suggested that increasing the H_{PCM} suppressed the convection of the liquid PCM in the early stage of the heat release, and prevented the aforementioned adverse solidification of the PCM.

In summary, the changes of the local temperature in the HSU in this study showed a tendency similar to that in the previous heat release experiments.[2] In the next section, we discuss the effects of the number of injection-nozzle holes, F, and H_{PCM} on the heat release performance. In other words, we investigated whether increasing the number of injection-nozzle holes and H_{PCM} would prevent drift flow of the HTO and the adverse solidification of the PCM for each F.

3.2. Heat Release Performance

As indices for the heat release performance, we defined the temperature effectiveness θ, which indicated the dimensionless performance of a heat exchanger, the heat exchange rate q, and the average values of these parameters during latent heat release, namely, $\theta_{av,l}$ and $q_{av,l}$. Eqs. (1)–(4) show the definitions. These index and analysis methods were similar to those used in the previous study.[2]

$$\theta = \frac{T_{in} - T_{out}}{T_{in} - T_m} \quad \text{..... (1)}$$

$$q = F\rho_{HTO}C_{P,HTO}(T_{in} - T_{out}) - q_{Loss} \quad \text{..... (2)}$$

Here, ρ_{HTO} and $C_{P,\,HTO}$ are the density and specific heat capacity of the HTO, respectively, and q_{Loss} is the heat loss from the HSU wall. q_{Loss} was calculated as the average of the heat losses measured by the six heat-flow meters on the wall of the HSU.

$$\theta_{av,l} = \frac{1}{t_{f,l} - t_{s,l}} \int_{t_{s,l}}^{t_{f,l}} \theta dt \quad \text{..... (3)}$$

$$q_{av,l} = \frac{1}{t_{f,l} - t_{s,l}} \int_{t_{s,l}}^{t_{f,l}} q dt \quad \text{..... (4)}$$

Here, $t_{s,l}$ and $t_{f,l}$ are the start and end times of the latent heat release, respectively. $t_{s,l}$ is defined as the time when T_{out} reached T_m. The period of the latent heat release was determined on the basis of the accumulated amount of heat, where $t_{f,l}$ is the time when the latent heat of the PCM was stored. Then, Eq. (5) was integrated over $t_{f,l}$.

$$M_{PCM}L = \int_{t_{s,l}}^{t_{f,l}} q dt \quad \text{..... (5)}$$

Here, M_{PCM}, and L are the mass of the PCM in the HSU and the latent heat of the PCM, respectively.

In addition, the LHS ratio η_l was calculated using Eq. (6).

$$\eta_l = \frac{1}{M_{PCM}L} \int_{t_{s,l}}^{t} q dt \quad \text{..... (6)}$$

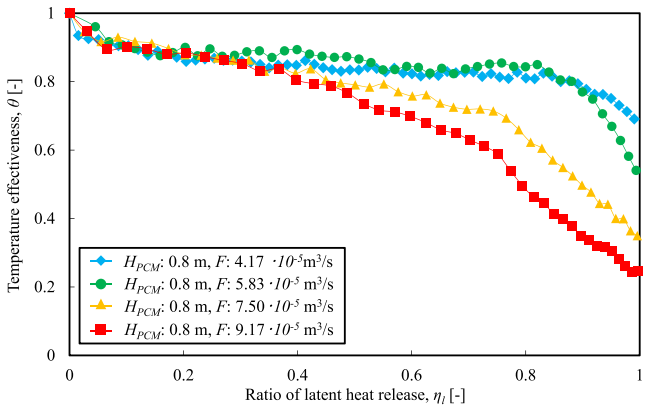

Fig. 5. Changes in temperature effectiveness θ with latent heat release ratio η_l under condition of constant H_{PCM}: 0.8 m and different F. The range of F is 4.17·10^{-5} m^3/s ≤ F ≤ 9.17 ·10^{-5} m^3/s. It should be noted that an increase in η_l indicates the progress of the latent heat release and a decrease in liquid PCM. (Online version in color.)

Figure 5 shows the changes in θ_l with respect to η_l under the conditions of a constant H_{PCM} of 0.8 m and different values of F. The range of F was 4.17·10^{-5} m^3/s ≤ F ≤ 9.17·10^{-5} m^3/s. Here, an increase in η_l indicates progress in the latent heat release, along with a decrease in the liquid PCM zone and an increase in the solid PCM. Under all the conditions, θ_l gradually decreased with an increase in $\eta_{r,l}$ and then

abruptly decreased at a value of $\eta_{r,l}$ greater than 0.7. Under the conditions of F: $4.17\cdot10^{-5}$ m^3/s and $5.83\cdot10^{-5}$ m^3/s, the decrease rates of θ_l with an increase in η_l were low. Therefore high θ_l over 0.8 were kept up to η_l over 0.8. On the other hand, under the conditions of F: $7.50\cdot10^{-5}$ m^3/s and $9.17\cdot10^{-5}$ m^3/s, the decrease rates of θ_l with an increase in η_l were higher than those for lower F. In our previous report,[2] we reported that a uniform HTO flow has a beneficial influence on the heat release performance, especially under the condition of a lower F. As examples, Refs. 1)–3) in Table 3 correspond to this condition. We also suggested that, under the condition of a higher F, the HTO drift flow and adverse solidification such as the liquid PCM becoming enclosed in the solid PCM, which were mentioned above in 3.1, caused a poor heat release performance. Similar phenomena occurred in this study, although the conditions such as the number of nozzles and H_{PCM} were different from those of the previous study.[2]

Figure 6 shows the changes in the heat exchange rate during the latent heat release, q_l, with the latent heat release ratio η_l, under the conditions of a constant H_{PCM} of 0.8 m and different values of F. The range of F was $4.17\cdot10^{-5}$ m^3/s $\leq$ F $\leq$ $9.17\cdot10^{-5}$ m^3/s. Higher q_l values were observed under the conditions of the larger F, up to about an η_l of 0.8. On the other hand, the q values for F: $7.50\cdot10^{-5}$ m^3/s and $9.17\cdot10^{-5}$ m^3/s abruptly decreased from η_l over about 0.8, and values smaller than those under the condition of a smaller F were observed. Under the condition of a high η_l, in other words, the range where a large quantity of liquid PCM remained, an increase in F greatly affected the acceleration of the heat exchange rate. On the other hand, in the range of large values for η_l, in other words, the range where little liquid PCM remained, the aforementioned HTO drift flow and adverse solidification strongly affected the heat transfer and, as a result, q_l rapidly decreased.

Figure 7 shows the variation in the average temperature effectiveness during the latent heat release, $\theta_{av,l}$ with the different values of F and H_{PCM} used in this study. To investigate the effect of the number of injection nozzles on the heat release performance, the results of the previous study[2] (see Table 3, Refs. 1)–6), F: $4.17\cdot10^{-5}$ m^3/s–$7.50\cdot10^{-5}$ m^3/s, H_{PCM}: 0.6 m, number of nozzle holes: 9, D_n: 3.0 φ) were also plotted with a schematic diagram of the injection nozzles. First, similar $\theta_{av,l}$ values were observed for each F at different values of H_{PCM}. Second, high $\theta_{r,av,l}$ values greater than 0.8 were observed for $F \leq 5.83\cdot10^{-5}$ m^3/s in this study. These were similar to the results of the previous study.[2] On the other hand, the present study kept a comparatively high $\theta_{r,av,l}$ greater than 0.7 under the condition of a higher F for $F \geq 5.83\cdot10^{-5}$ m^3/s, although the $\theta_{av,l}$ of the previous study abruptly decreased for a higher F.

These results indicate that an increase in the number of the injection-nozzle holes can 1) accelerate the uniform distribution of the HTO in the liquid PCM and prevent the drift flow of the HTO and adverse solidification of the PCM, and 2) spread the heat transfer area of the HTO droplets. This effectively improves the heat release performance.

Figure 8 shows the variation in the average heat exchange rate during the latent heat release, $q_{av,l}$, with the different values of F and H_{PCM} used in this study. The results of the previous study (see Table 3, Refs. 1)–6), F: $4.17\cdot10^{-5}$ m^3/s–$7.50\cdot10^{-5}$ m^3/s, H_{PCM}: 0.6 m, number of nozzle holes: 9, D_n: 3.0 φ) were also plotted with a schematic diagram of the injection nozzles. First, $q_{av,l}$ increased with an increase in F

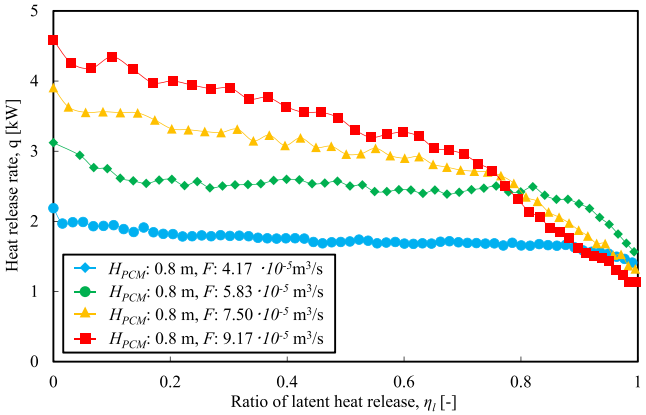

Fig. 6. Changes in heat exchange rate q with latent heat release ratio η_l under condition of constant H_{PCM}: 0.8 m and different F. The range of F is $4.17\cdot10^{-5}$ m^3/s $\leq F \leq 9.17\cdot10^{-5}$ m^3/s. It should be noted that an increase in η_l indicates the progress of the latent heat release and a decrease in liquid PCM. (Online version in color.)

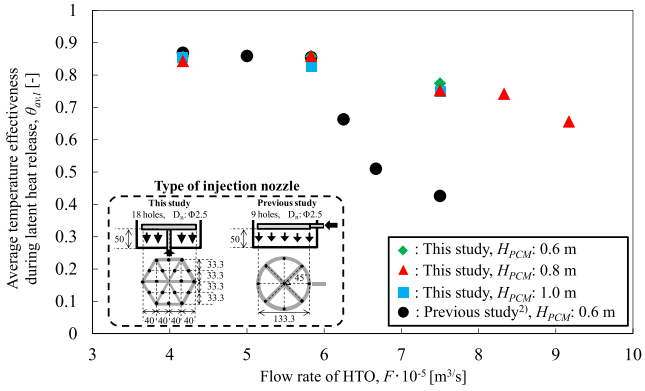

Fig. 7. Variation in average temperature effectiveness during latent heat release, $\theta_{av,l}$ with different F and H_{PCM} in this study, and those of previous study[2] (Refs. 1)–6), F: 4.17–$7.50\cdot10^{-5}$ m^3/s, H_{PCM}: 0.6 m, number of nozzle holes: 9, D_n: 3.0 φ), together with schematic diagram of injection nozzles used in this study and previous study. (Online version in color.)

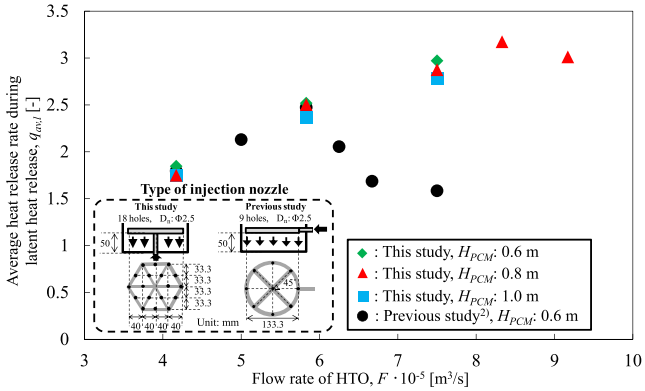

Fig. 8. Variation in average heat release rate during latent heat release $q_{av,l}$ with different F and H_{PCM} in this study, and those of previous study [2] (Refs. 1)–6), F: 4.17–$7.50\cdot10^{-5}$ m^3/s, H_{PCM}: 0.6 m, number of nozzle holes: 9, D_n: 3.0 φ), together with schematic diagram of injection nozzles used in this study and previous study. (Online version in color.)

up to $8.33 \cdot 10^{-5}$ m^3/s, and q had similar values at each F for different H_{PCM}. This clearly suggested that the heat release rate more strongly depended on F than H_{PCM}, which is related to the holding period of the HTO in the liquid PCM. In a comparison of the results of the present and previous studies,[2] the $q_{av,l}$ of the previous study abruptly decreased under the condition of a higher F, but the $q_{av,l}$ of the present study was proportional to F, even for high F values greater than $5.83 \cdot 10^{-5}$ m^3/s. When F was $7.50 \cdot 10^{-5}$ m^3/s, the $q_{av,l}$ value of the present study was double that of the previous study.

In conclusion, we achieved a remarkable improvement in the heat release performance of a DCHEX of the vertical cylindrical tank type.

4. Conclusions

In this study, we examined the effects of the height of the PCM, the flow rate of the HTO, and an increase in the number of injection-nozzle holes on the temperature effectiveness θ and heat exchange rate q for a DCHEX of the vertical cylindrical tank type. The following are the major conclusions.

(1) The temperature histories in this study were similar to those of the previous study. A higher F was likely to cause an HTO drift flow and adverse solidification of the PCM.

(2) H_{PCM} contributed less to the heat release performance compared to the great contribution of F.

(3) Increasing the number of injection-nozzle holes could improve the heat release performance, especially under the condition of a high F *because* 1) it accelerated the uniform distribution of the HTO in the liquid PCM and prevented the HTO drift flow and adverse solidification of the PCM, and 2) it spread the heat transfer area of the HTO droplets.

In conclusion, we achieved a remarkable improvement in the heat release performance of a DCHEX of the vertical cylindrical tank type.

Acknowledgment

This research was partially supported by the project "CO_2 Ultimate Reduction in Steelmaking Process by Innovative Technology for Cool Earth 50" of the New Energy and Industrial Technology Development Organization, Japan.

Nomenclature

A: *Cross-sectional area of HSU* (m^2)
$C_{P,\,HTO}$: Specific heat of HTO (kJ/kg·K)
$C_{P,\,PCM,\,l}$: Specific heat of liquid PCM (kJ/kg·K)
$C_{P,\,PCM,\,s}$: Specific heat of solid PCM (kJ/kg·K)
D_n: Diameter of hole of inlet nozzle (mm)
F: Flow rate of HTO (m^3/s)
H_{PCM}: Height of PCM in HSU (m)
L: Latent heat of PCM (kJ/kg)
M_{HTO}: Mass of HTO in HSU (kg)
M_{PCM}: Mass of PCM in HSU (kg)
q: Heat release rate (kW)
$q_{av,\,l}$: Average heat release during latent heat release (kW)
Re_n: Reynolds number of inlet HTO ($\rho_{HTO} v_n D_n / \mu_{HTO}$) (–)
V_{PCM}: Volume of PCM in HSU (m^3)
$t_{s,\,l}$: Time at which latent heat release begins (s)
$t_{f,\,l}$: Time at which latent heat release ends (s)
T_{in}: Temperature of inlet HTO (K)
T_m: Melting point of PCM (K)
T_{out}: Temperature of outlet HTO (K)
v_c: Superficial velocity of HTO in HSU (F/A) (m/s)
v_n: Inlet velocity of HTO (m/s)
θ: Temperature effectiveness (–)
$\theta_{av,\,l}$: Average temperature effectiveness during latent heat release (–)
ρ_{HTO}: Density of HTO (kg/m^3)
μ_{HTO}: Viscosity of HTO (kg/m·s)
η_l: Latent heat release ratio (–)

Abbreviation

DCHEX: Direct-contact heat exchanger
HTO: Heat transfer oil
HSU: Heat storage unit
LHS: Latent heat storage
PCM: Phase change material
TES: Thermal energy storage

REFERENCES

1) T. Akiyama: *ISIJ Int.*, **50** (2010), 1227.
2) T. Nomura, M. Tsubota, T. Oya, N. Okinaka and T. Akiyama: *Appl. Therm. Eng.*, **61** (2013), 28.
3) S. Guo, H. Li, J. Zhao, X. Li and J. Yan: *Appl. Energ.*, **113** (2013), 1416.
4) A. Kaizawa, H. Kamano, A. Kawai, T. Jozuka, T. Senda, N. Maruoka and T. Akiyama: *Energ. Conver. Manag.*, **49** (2008), 698.
5) A. Kaizawa, H. Kamano, A. Kawai, T. Jozuka, T. Senda, N. Maruoka, N. Okinaka and T. Akiyama: *ISIJ Int.*, **48** (2008), 540.
6) A. Kaizawa, N. Maruoka, A. Kawai, H. Kamano, T. Jozuka, T. Senda and T. Akiyama: *Heat Mass. Transf.*, **44** (2008), 763.
7) S. Tagashira, Y. Ito, Y. Murakami, Y. Higashi and K. Takahashi: *KOBELCO Eco-Solutions Eng. Rep.*, **2** (2006), 36.
8) H. Inaba and S.-I. Morita: *Int. J. Heat Mass Transf.*, **39** (1996), 1797.
9) K. Nagano, S. Takeda, T. Mochida and K. Shimakura: *Appl. Therm. Eng.*, **24** (2004), 2131.
10) H. Inaba and K. Sato: *Nippon Kikai Gatsukai Ronbunshu* (*B*), **62** (1996), 325.
11) H. Inaba and K. Sato: *Nippon Kikai Gatsukai Ronbunshu* (*B*), **63** (1997), 267.
12) A. Saito, Y. Utaka, K. Okuda and K. Katayama: *Nippon Reito Kyokai Ronbunshu*, **3** (1986), 43.
13) A. Saito, Y. Utaka, K. Okuda and K. Katayama: *Nippon Reito Kyokai Ronbunshu*, **3** (1986), 51.
14) T. Nomura, T. Oya, N. Okinaka and T. Akiyama: *ISIJ Int.*, **50** (2010), 1326.
15) T. Nomura, M. Tsubota, T. Oya, N. Okinaka and T. Akiyama: *Appl. Therm. Eng.*, **50** (2013), 26.
16) A. Horibe, Y. Jang, N. Haruki and K. Takahashi: *Therm. Sci. Eng.*, **21** (2013), 83.
17) H. Nogami, K. Ikeuchi and K. Sato: *ISIJ Int.*, **50** (2010), 1270.
18) T. Nomura, M. Tsubota, A. Sagara, N. Okinaka and T. Akiyama: *Appl. Therm. Eng.*, (2013).
19) M. Kakiuchi, M. Yamazaki, M. Yabe, S. Chihara, Y. Terunuma, Y. Sakata and T. Usami: IEA Annex 10-PCMs and Chemical Reactions for Thermal Energy Storage, 2nd Workshop, IEA, Paris, (1998), 11.